The stochastic gravitational wave background - power-law modelling and sources

Anna Kormu

University of Helsinki, Finland

September 5, 2018

Abstract

The cosmological stochastic gravitational wave background consists of relic gravitational waves from the very early universe. In this report we will take a brief look at two of the possible sources, cosmological first-order phase transitions and cosmic strings. Both sources lie in the detection sensibility range of LISA. We will also take a look at backgrounds that can be modelled with a power-law and recreate power-law integrated sensitivity curves for LISA and other ground-based detectors such as LIGO.

Contents

1 Introduction **2**

2 The cosmological stochastic GW background **2**

3 Power-law integrated sensitivity curves **4**

3.1 LISA 5

3.2 Ground-based detectors 6

4 GWs from phase transitions **7**

4.1 Sound waves 9

4.2 Magnetohydrodynamic turbulence 9

4.3 GW spectra 10

5 GWs from cosmic strings **10**

6 Conclusions **15**

A Appendix **17**

1 Introduction

Gravitational waves (GWs) are perturbations in the curvature of space-time that are created when objects accelerate. Gravitational waves were first directly detected in 2015 when LIGO (The Laser Interferometer Gravitational-Wave Observatory) observed a signal from two black holes merging [1]. GWs are predicted by Einstein's theory of general relativity, but the concept was first proposed by French physicist Henri Poincaré in 1905 [2].

However, LIGO is not the only detector for GW detection. The International Pulsar Timing Array (IPTA) collaboration is currently looking at the other end of the GW frequency spectrum ($f \sim 10^{-9}$ to 10^{-8} Hz) with widely distributed millisecond pulsars [3]. A sensitivity for a detection is expected to be reached with the SKA (Square Kilometre Array) Telescope that is currently moving towards its construction phase [4].

There are limitations with Earth-based detectors such as seismic noise that prohibits them going to longer wavelengths. Therefore, we must consider also building space-based detectors in addition to the emerging third generation of ground-based detectors, Cosmic Explorer (CE) and Einstein Telescope (ET). This is where detectors such as LISA (Laser Interferometer Space Antenna), BBO (Big Bang Observer) and DECIGO (Deci-Hertz Interferometer Gravitational wave Observatory) step in, see Fig. 1.

In this report we will focus on the stochastic cosmological GW background and in its possible sources. The stochastic background consists of multiple independent sources that when combined form a background of gravitational waves from the early universe. The stochastic background is therefore sought after for the information it could provide of the events from the very early universe. Namely probe the cosmology before Big Bang nucleosynthesis, thus offering a new source of information for high energy physics research [5].

2 The cosmological stochastic GW background

Like introduced in the previous section, the cosmological stochastic GW background consists of relic GWs from the very early universe. These relic GWs originate from different independent cosmological sources. The background is isotropic, stationary and unpolarized leading to a conclusion that its main property is the frequency spectrum the GWs produce [5]. In this section we will briefly go through how to characterise this stochastic background.

The fractional energy density of the GW with respect to the total energy density of the

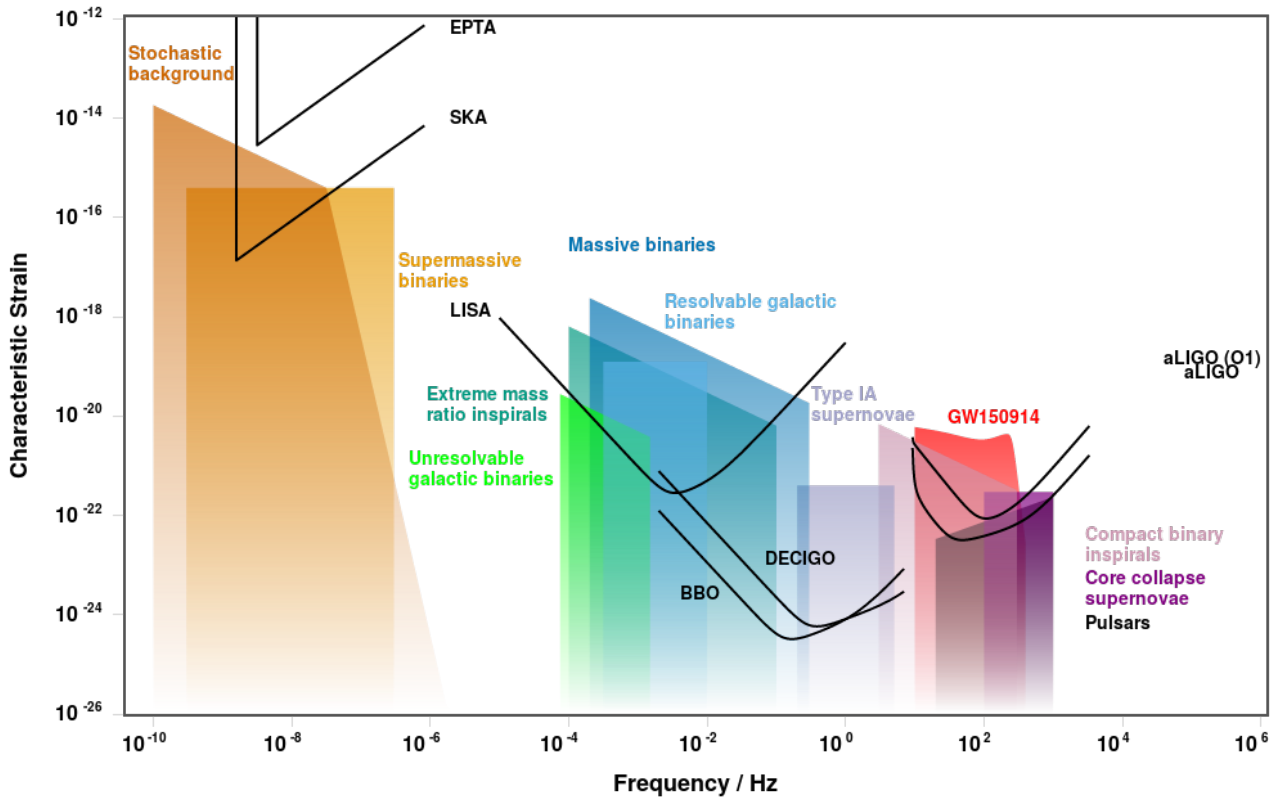

Figure 1: The sensitivity curves of current and future detectors. The highlighted areas are regions where the different sources may produce GWs. Source: `http://gwplotter.com/`

universe today is

$$\Omega_{GW}(f) = \frac{1}{\rho_c}\frac{d\rho_{\rm GW}}{d\,\log\,f}, \tag{1}$$

where $\rho_{\rm GW}$ is the energy density of stochastic background of cosmological origin and ρ_c is the critical energy density of the universe defined as

$$\rho_c = \frac{3H_0^2}{8\pi G}, \tag{2}$$

where G is Newton's constant and H_0 is the Hubble constant. $H_0 = h_0 \times 100$ km/(s $\times$ Mpc) where the value h_0 represents the experimental uncertainty. We have set $h_0 = 0.7$. We also express the intensity of the stochastic GW background as $h_0^2\Omega_{\rm GW}$ in order to eliminate the uncertainty that comes with using h_0 [5].

We can also express quantity $\Omega_{\rm GW}$ with the help of characteristic amplitude of the stochastic background $h_c(f)$ as

$$\Omega_{\rm GW} = \frac{2\pi}{3H_0^2} f^2 h_c(f)^2. \tag{3}$$

The relationship between characteristic strain and the spectral density $S_h(f)$ is known to be [6]

$$h_c(f) = \sqrt{f S_h(f)}. \tag{4}$$

Thus, Eq. 1 can be also written as

$$\Omega_{\rm GW} = \frac{2\pi}{3H_0^2} f^3 S_h(f). \tag{5}$$

3 Power-law integrated sensitivity curves

In this report we will focus solely on stochastic backgrounds that can be modelled with a power-law. Integrating over frequency, as well as time, increases the detection sensitivity of the stochastic background. The method for creating these curves is introduced in Ref. [6]. We call these curves that take into account the increased sensitivity of the detectors power-law integrated curves. We now produce these sensitivity curves for different durations of LISA mission as well as ground-based detectors CE and TE. We also construct the power-law integrated curve for LIGO. Since LIGO consists of two detectors (Hanford and Livingston sites) we need to take into account the overlap reduction function. We go briefly through the method of creating these curves.

The detectability of a GW signal can be estimated with a signal-to-noise ratio

$$SNR = \sqrt{t \int_{f_{\rm min}}^{f_{\rm max}} {\rm d}f \left[\frac{h^2 \Omega_{\rm GW}(f)}{h^2 \Omega_{\rm sens}} \right]^2}\,, \tag{6}$$

where t is the duration of the mission, $\Omega_{\rm sens}$ is the sensitivity of the detector [7].

We will assume that the stochastic gravitational wave background can be modelled with a power-law,

$$\Omega_{\rm GW} = \Omega_\beta \left(\frac{f}{f_{\rm ref}} \right)^\beta, \tag{7}$$

where β is the spectral index and $f_{\rm ref}$ is the reference frequency that depends on the detector in question. However, the value is arbitrary and does not affect the computation.

For a fixed value of SNR and t we now have the following equation

$$\Omega_\beta = \frac{SNR}{\sqrt{t}} \left[\int_{f_{\min}}^{f_{\max}} \mathrm{d}f \frac{(f/f_{\mathrm{ref}})^{2\beta}}{\Omega^2_{\mathrm{sens}}(f)} \right]^{-1/2}, \tag{8}$$

where the integration limits ranging from $f_{\min}$ to $f_{\max}$ determine the bandwith of the detector.

It is now straightforward to compute Ω_β for a given value of SNR, where β is a set of 50 values in the range $\beta = \{-8, .., 8\}$. We now get an envelope of curves using Eq. 7, see Fig. 2 for reference. The final curve is composed of the maximum values of each curve, or more formally by [6]

$$\Omega_{\mathrm{PL}}(f) = \max_\beta \left[\Omega_\beta \left(\frac{f}{f_{\mathrm{ref}}} \right)^\beta \right]. \tag{9}$$

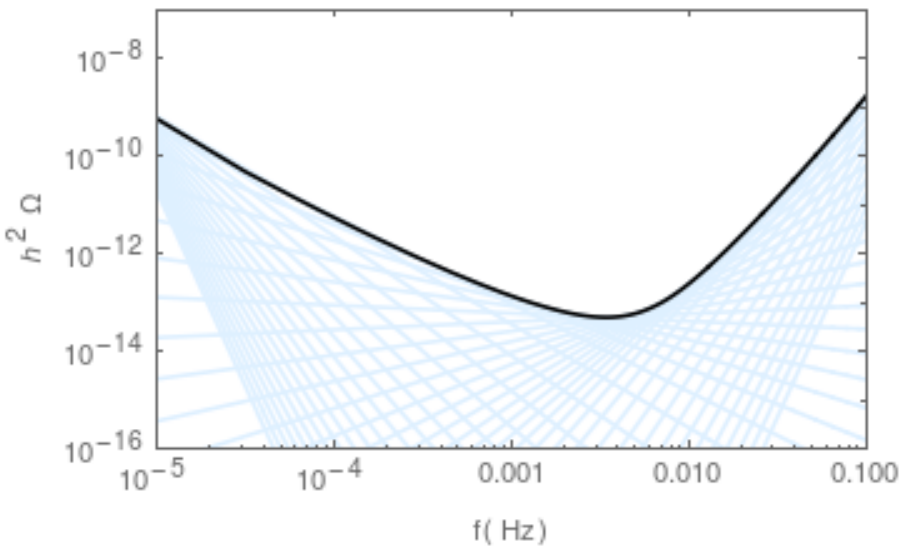

Figure 2: The power-law integrated curves are in light blue and the known LISA power-law curve is in black. The $SNR = 20$ and duration of the mission $t = 5$ years.

3.1 LISA

The LISA mission is currently expected to launch in 2034 and it will be the very first gravitational wave detector in space. LISA will be a triangular configuration consisting of three spacecraft with an arm-length of 2.5 million km and it will follow Earth from a distance of 50 million km [8].

We have performed an analysis of the sensitivity that can be acquired varying the duration of the mission and the value of SNR, see Fig. 3. As can be clearly seen, all of the power-law curves vary only slightly in their detection sensitivity.

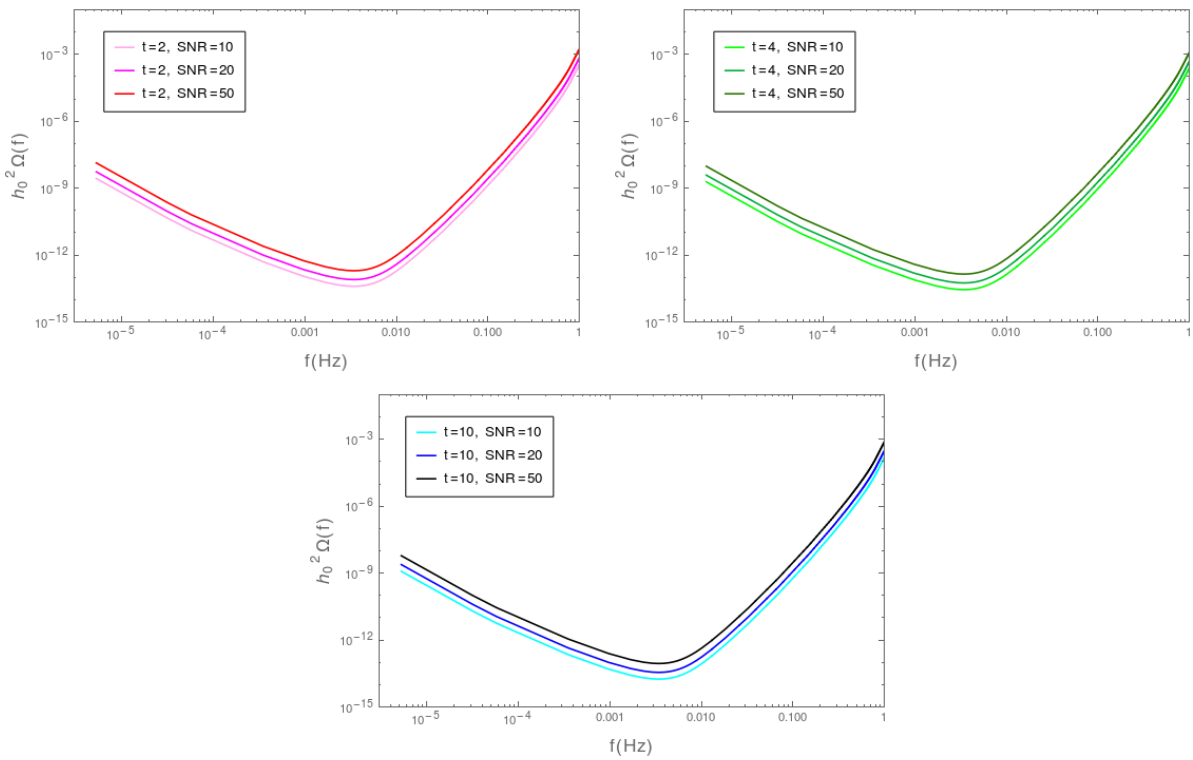

Figure 3: The produced sensitivity curves for LISA using the power-law integrated method. We vary the values of SNR and t in years.

3.2 Ground-based detectors

Utilizing the same method from previous section for ground-based detectors, such as CE and ET, we can now produce the power-law integrated sensitivity curves. The process does not differ for CE and ET, but for detectors that consist of more than one detector one needs to determine overlap reduction function that is specific for the detector in question.

To determine the power-law integrated sensitivity curves for LIGO (Fig. 5), we have take into account the fact that there are two detectors. In this case we have to include the overlap reduction function for LIGO in Eq. 6 [5]. Thus Eq. 8 becomes

$$\Omega_\beta = \frac{SNR}{\sqrt{t}} \left[\int_{f_{\rm min}}^{f_{\rm max}} {\rm d}f \, \left(\frac{\gamma F_{12}(f/f_{\rm ref})^\beta}{\Omega_{\rm sens}} \right)^2 \right]^{-1/2} , \tag{10}$$

where $F_{12} = \frac{2}{5}$ in the case of two detectors and γ is given as a function of frequency in Fig. 4 [5, 6].

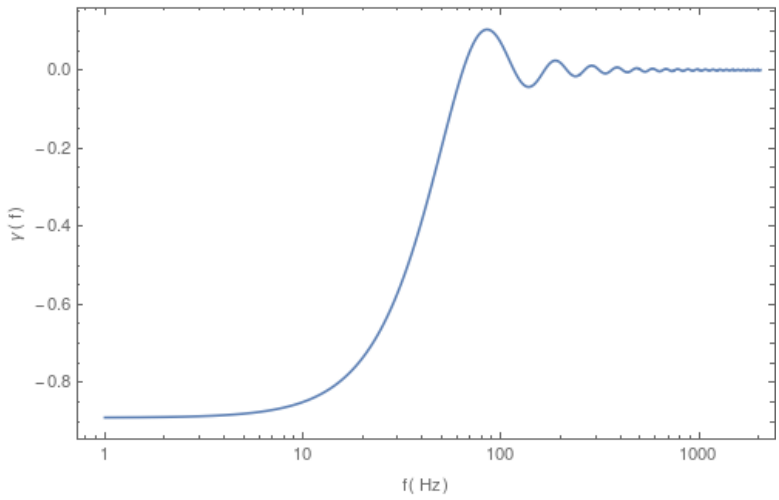

Figure 4: The normalised overlap reduction function for LIGO.

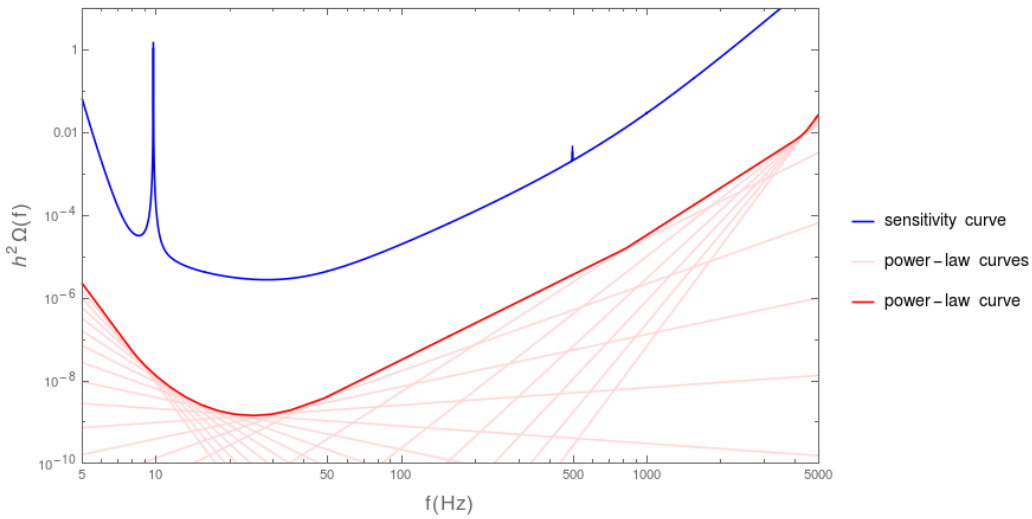

Figure 5: Powe-law integrated sensitivity curve for LIGO, $SNR = 10$ and $t = 4$ years.

4 GWs from phase transitions

One source of a cosmological stochastic GW background are the first order cosmological phase transitions (PTs) that are predicted by many beyond the Standard Model (SM) theories. These PTs occur when there coexist two local minima, one is in the false vacuum state and the other in the true vacuum. The field is initially in the false vacuum, and bubbles of the true vacuum state then nucleate. These bubbles expand and collide which results in gravitational waves, see Fig. 6 [6].

One of the most attractive scenarios for cosmological PTs to occur is the electroweak symmetry breaking. However, in the SM the transition is a crossover instead of a first-order transition [9]. Nonetheless, in the extensions of SM a electroweak first-order PT still remains as a possibility and models where the cosmological PT is not tied to the electroweak scale exist. The background from a first order electroweak PT might the detectable for LISA and the next generation of ground-based detectors [7, 10]. For a more detailed review of the GWs from cosmological PTs see Ref. [11].

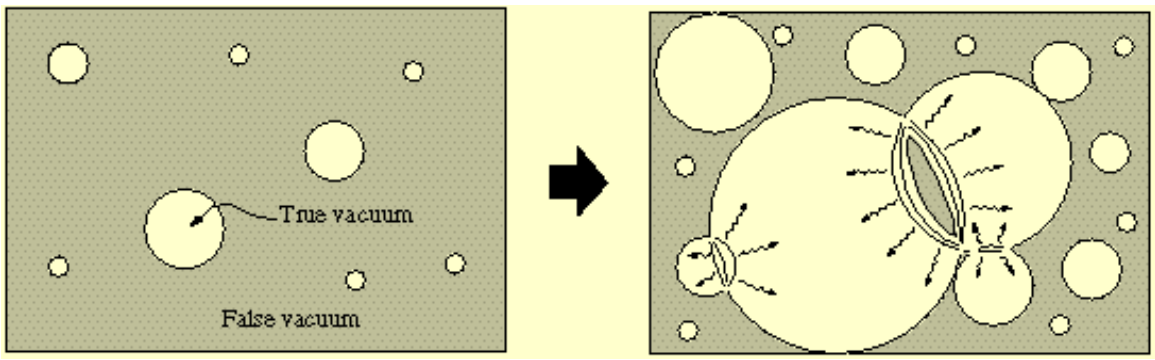

Figure 6: Bubbles nucleating from the false vacuum into the true vacuum state. Source: `http://www.ctc.cam.ac.uk/`

The GW background from PTs has three main processes that produce GWs, the importance of a contribution from a certain process depends on the model in question. The contributions are from bubble wall collisions, sound waves in the plasma and magnetohydrodynamic (MHD) turbulence. Combining these contributions we get

$$h^2\Omega_{\rm GW} = h^2\Omega_{\Phi} + h^2\Omega_{\rm sw} + h^2\Omega_{\rm turb} \tag{11}$$

We will now take a closer look at one of the widely studied cases, non-runaway bubbles. In this case Eq. 11 becomes

$$h^2\Omega_{\rm GW} \simeq h^2\Omega_{\rm sw} + h^2\Omega_{\rm turb}. \tag{12}$$

The velocity of the bubble walls is relativistic and thus the contribution from collisions i.e. the scalar field is negligible [7].

4.1 Sound waves

The bubble wall proceeds to move in the plasma creating sound waves. This contribution can be modelled as

$$h^2\Omega_{sw}(f) = 2.65 \times 10^{-6} \left(\frac{H_*}{\beta}\right) \left(\frac{\kappa_v \alpha}{1+\alpha}\right)^2 \left(\frac{100}{g_*}\right)^{1/3} v_w S_{\rm sw}(f), \tag{13}$$

where T_* is the temperature at time t_* when the GWs are produced, β is the inverse time duration of the PT, H_* is the Hubble parameter at T_*, v_w is the bubble wall velocity, g_* is the number of degrees of freedom and α is defined as the ratio of vacuum energy density to the radiation bath.

In the case of non-runaway bubbles, the fraction of latent heat converted into bulk motion is

$$\kappa_v \simeq \alpha(0.73 + 0.083\sqrt{\alpha} + \alpha)^{-1} \qquad v_w \sim 1. \tag{14}$$

The spectral shape $S_{\rm sw}(f)$ is defined as

$$S_{\rm sw}(f) = \left(\frac{f}{f_{\rm sw}}\right)^3 \left(\frac{7}{4 + 3(f/f_{\rm sw})^2}\right)^{7/2} \tag{15}$$

where $f_{\rm sw}$ is the peak frequency that is defined as

$$f_{\rm sw} = 1.9 \times 10^{-5}\ {\rm Hz} \frac{1}{v_w} \left(\frac{\beta}{H_*}\right) \left(\frac{T_*}{100\ {\rm GeV}}\right) \left(\frac{g_*}{100}\right)^{1/6}. \tag{16}$$

4.2 Magnetohydrodynamic turbulence

In addition to creating sound waves, percolation can also create MHD turbulence in the fully ionised plasma. The MHD contribution in the GW background can be expressed as follows

$$h^2\Omega_{\rm turb}(f) = 3.35 \times 10^{-4} \left(\frac{H_*}{\beta}\right) \left(\frac{\kappa_{\rm turb} \alpha}{1+\alpha}\right)^{3/2} \left(\frac{100}{g_*}\right)^{1/3} v_w S_{\rm turb}(f). \tag{17}$$

The fraction of latent heat converted to MHD turbulence is

$$\kappa_{\rm turb} = \epsilon \kappa_v, \tag{18}$$

where ϵ is the fraction that is turbulent. This determines how big of a contribution MHD turbulence has on the GW background. For the sake of being consistent with Ref. [7] we have set $\epsilon = 0.05$.

The spectral shape has an analytical solution of the form

$$S_{\rm turb}(f) = \frac{(f/f_{\rm turb})^3}{[1+(f/f_{\rm turb})]^{11/3}\,(1+8\pi f/h_*)}, \tag{19}$$

where the equation depends on the Hubble rate h_* and $f_{\rm turb}$ is the peak frequency,

$$h_* = 16.5\times 10^{-6}\ {\rm Hz}\left(\frac{T_*}{100\ {\rm GeV}}\right)\left(\frac{g_*}{100}\right)^{1/6}, \tag{20}$$

$$f_{\rm turb} = 2.7\times 10^{-5}\ {\rm Hz}\frac{1}{v_w}\left(\frac{\beta}{H_*}\right)\left(\frac{T_*}{100\ {\rm GeV}}\right)\left(\frac{g_*}{100}\right)^{1/6}. \tag{21}$$

4.3 GW spectra

Now using Eqs. 12, 13 and 17 we can write down the theoretical prediction for GWs from cosmological PTs and compare it to the LISA power-law sensitivity curve, see Fig. 7. We can clearly see that the larger the ratio β/H_* becomes the weaker the occurring phase transition becomes and thus results in a weaker signal. However, all the considered scenarios fall to the sensitivity range of LISA.

5 GWs from cosmic strings

Cosmic strings are thin and line-like objects that may have formed in the early universe during phase transitions, see Fig. 8. They remain a viable prediction in many of the beyond the standard model theories [12]. Cosmic strings can be thought of as infinitely long objects that cross the horizon but they can also form smaller loops [13]. Cosmic strings emit gravitational radiation and their emissions would be distinguishable in the stochastic gravitational wave background [14]. Both LISA and the IPTA collaboration may be able to probe the frequency spectrum where cosmic strings may produce GWs [15]. However, in this report we will only focus on GWs from cosmic string loops since their contribution is dominant. Let it also be stated that the model question is the Nambu-Goto model and for a review of field theory strings we refer the interested reader to Ref. [12].

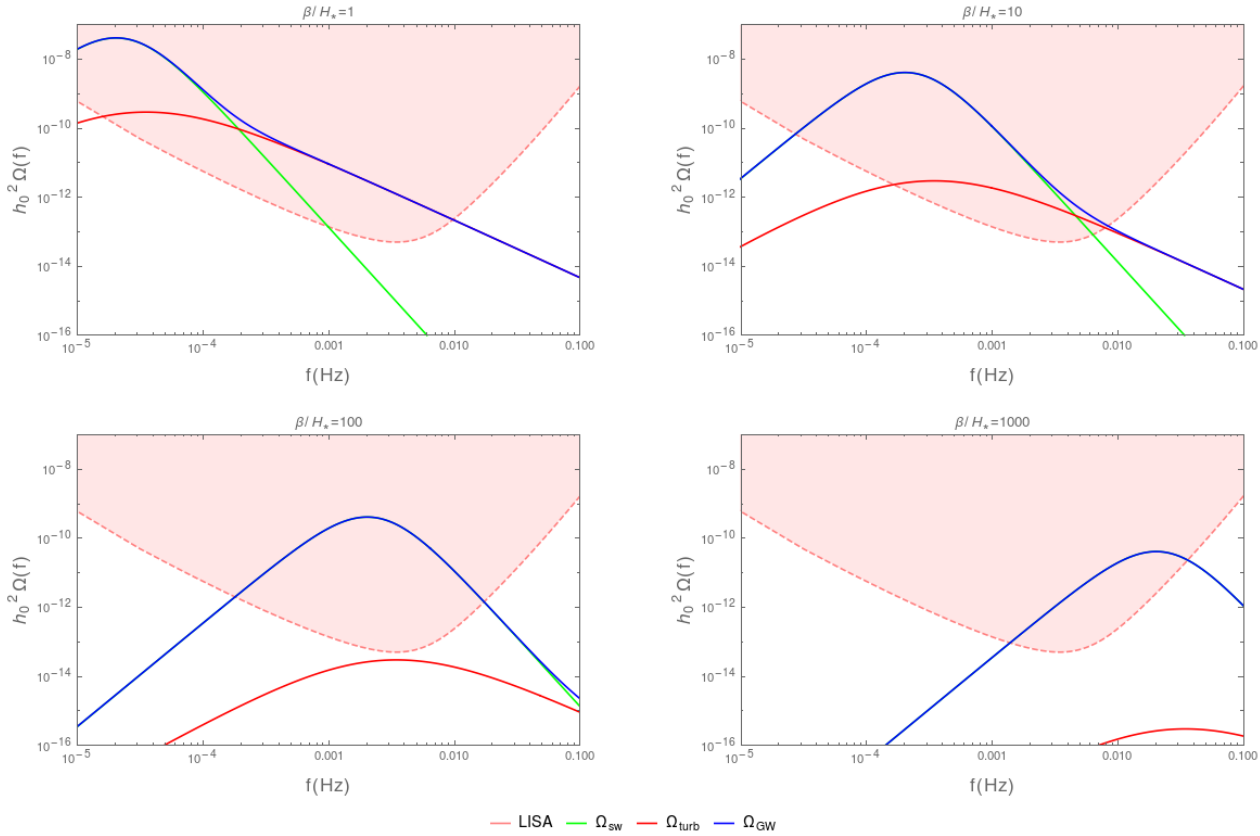

Figure 7: Non-runaway bubbles with different values of β/H_* while $T_* = 100$ GeV, $\alpha = 0.5$, $g_* = 106.75$ and $v_w = 0.95$. The green line is the contribution from sounds waves, red from MHD turbulence and envelope is blue. The LISA data and detecting sensitivity region is highlighted in red, we have assumed $SNR = 20$ and $t = 5$.

Cosmic strings, if they exist, are not a dominant contribution in the CMB measurements and thus the network has to exhibit scaling behaviour as the universe expands [12] [16]. Intercommuting and intersecting are important processes in achieving this scaling behaviour of the network, see Fig. 9. These processes create loops that oscillate, radiate and decay. The GW emission from loops can give rise to notable GW signal in the stochastic GW background. We will use the GW spectrum model reviewed in Refs. [17, 18] for the analysis of the GW background cosmic strings may produce. We assume that majority of the produced GWs are from the large loops, that while being less abundant in the network compared to smaller loops, are dominant. Smaller loops lose their energy due redshifting [18].

The length of the larger loops can be modelled with,

$$l_i = \alpha t_i, \tag{22}$$

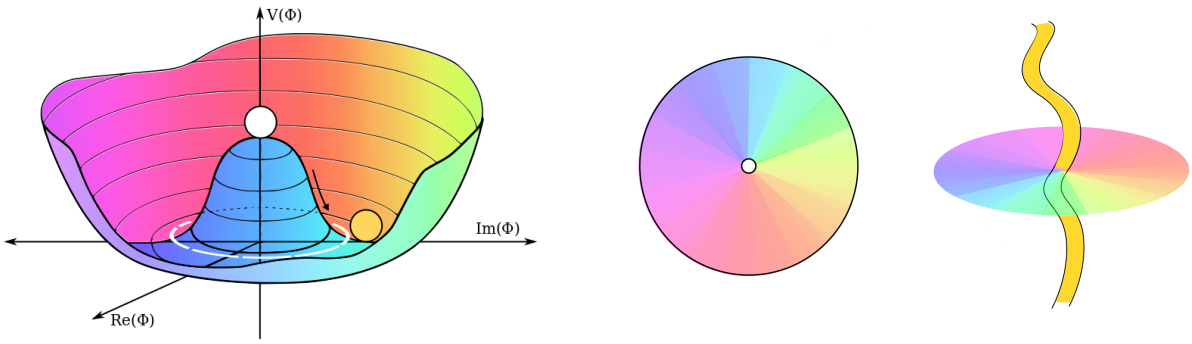

Figure 8: The Higgs field falls into its vacuum expectation value. The different colours represent the different orientations the Higgs field can fall into. In the core of the string the potential must have its peak value in order for the field to be continuous [13].

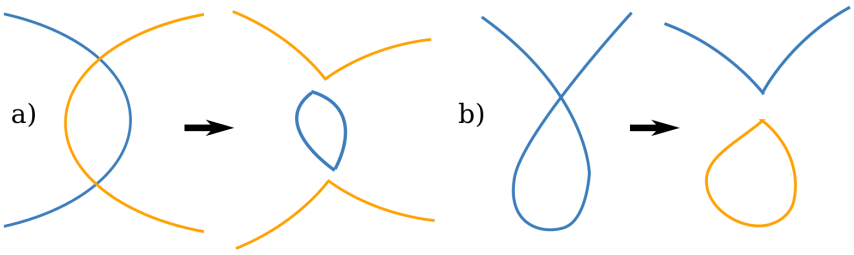

Figure 9: a) Two strings connecting and creating a loop and b) a string intercommuting with itself

where t_i is the time when the loop formed and the constant loop size parameter is set to $\alpha = 0.1$. It now follows that as the loop emits energy at constant rate the length of the loop as a function of time becomes

$$l(t) = \alpha t_i - \Gamma G\mu(t - t_i), \tag{23}$$

where $\Gamma = 50$ is a dimensionless constant and μ is the string tension of the cosmic string i.e. the energy stored per unit length. The most stringent limits for μ come from the IPTA collaboration.

The frequency of the emitted GW for a mode k is

$$f_{\text{emit}} = \frac{2k}{l} \qquad \text{where} \quad k = 1, 2, 3... \tag{24}$$

The frequency now redshifts as $a(t)^{-1}$ and thus we acquire the frequency as a function of

emission time $\tilde{t}$

$$f = \frac{a(\tilde{t})}{a(t_0)} \frac{2k}{\alpha t_i - \Gamma G\mu(\tilde{t} - t_i)}, \tag{25}$$

where t_0 is the current time, $\tilde{t}$ is the time when the GW signal was emitted and $a(t)$ is the cosmological scale factor.

By inverting Eq. 25 we acquire the function for the loop formation time

$$t_i^k(\tilde{t}, f) = \frac{1}{\alpha + \Gamma G\mu} \left[\frac{2k}{f} \frac{a(\tilde{t})}{a(t_0)} + \Gamma G\mu \tilde{t} \right] \tag{26}$$

The GW contribution from cosmic strings thus takes the form of

$$\Omega_{GW} = \sum_k \Omega_{GW}^{(k)}(f) \tag{27}$$

$$\begin{aligned} \Omega_{GW}^{(k)}(f) &= \frac{1}{\rho_c} \frac{2k}{f} \frac{(0.1)\Gamma_k G\mu^2}{\alpha(\alpha + \Gamma G\mu)} \int_{t_F}^{t_0} \mathrm{d}\tilde{t} \, \frac{C_{eff}(t_i)}{t_i^4} \left[\frac{a(\tilde{t})}{a(t_0)} \right]^5 \left[\frac{a(t_i)}{a(\tilde{t})} \right]^3 \Theta(t_i^k - t_F) \\ &= \frac{1}{\rho_c} \frac{2k}{f} \frac{(0.1)\Gamma_k G\mu^2}{\alpha(\alpha + \Gamma G\mu)} \, \mathcal{I}(\tilde{t}, f), \end{aligned} \tag{28}$$

where t_F is the network formation time, $\Gamma_k = \Gamma/3.60k^{4/3}$ and C_{eff} is the loop emission factor that depends on the redshift factor n. We have set $C_{\text{eff,radiation}} = 5.4$ and $C_{\text{eff,matter}} = 0.39$ [18].

The mode $k = 1$ is dominant and thus we only sum over the first ten values of k and conclude that this approximation is accurate. The integration limits go from radiation domination to matter era thus we have to split the integral into parts. We consider the cases when both t_i and $\tilde{t}$ are in radiation domination, t_i is in radiation but $\tilde{t}$ in matter and the both in matter domination. Thus we arrive in the following equation for the integral,

$$\mathcal{I}(\tilde{t}, f) = \int_{t_{\mathrm{F}}}^{t_{\mathrm{Eq}}} \mathrm{d}\tilde{t} \; F_{\text{radiation}}(\tilde{t}, f) \quad + \quad \int_{t_{\mathrm{Eq}}}^{t_0} \mathrm{d}\tilde{t} \; F_{\text{matter}}(\tilde{t}, f), \tag{29}$$

where $F(\tilde{t}, f)$ is the integrand when $\tilde{t}$ is in radiation and matter era respectively. One must be careful with the scale factor ratios and note that t_i depends on the emission time.

Now it becomes evident, that using the model in question the GW contributuion from cosmic strings in detectable in the freaquency range of LISA as well as the upcoming ground-based

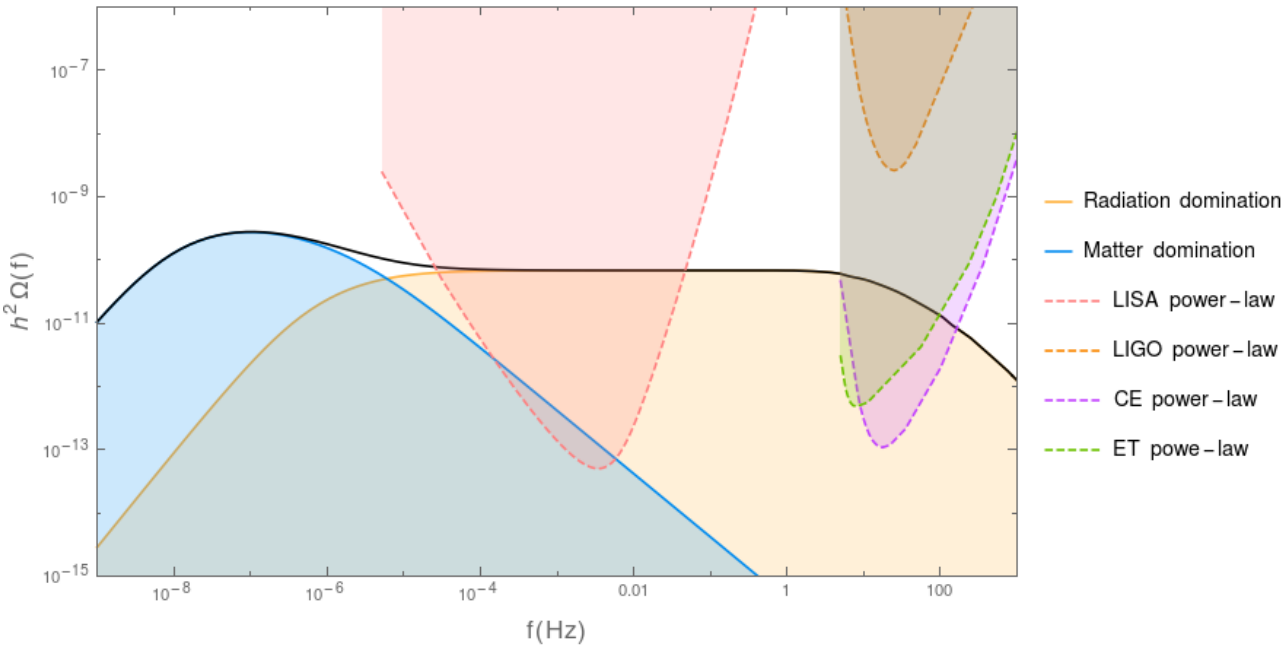

Figure 10: The black curve illustrates both radiation and matter contribution. We have set $T_{max} = 100$ GeV, $G\mu = 10^{-11}$. The LISA power-law curve corresponds to $SNR = 20$ and $t = 5$ years.

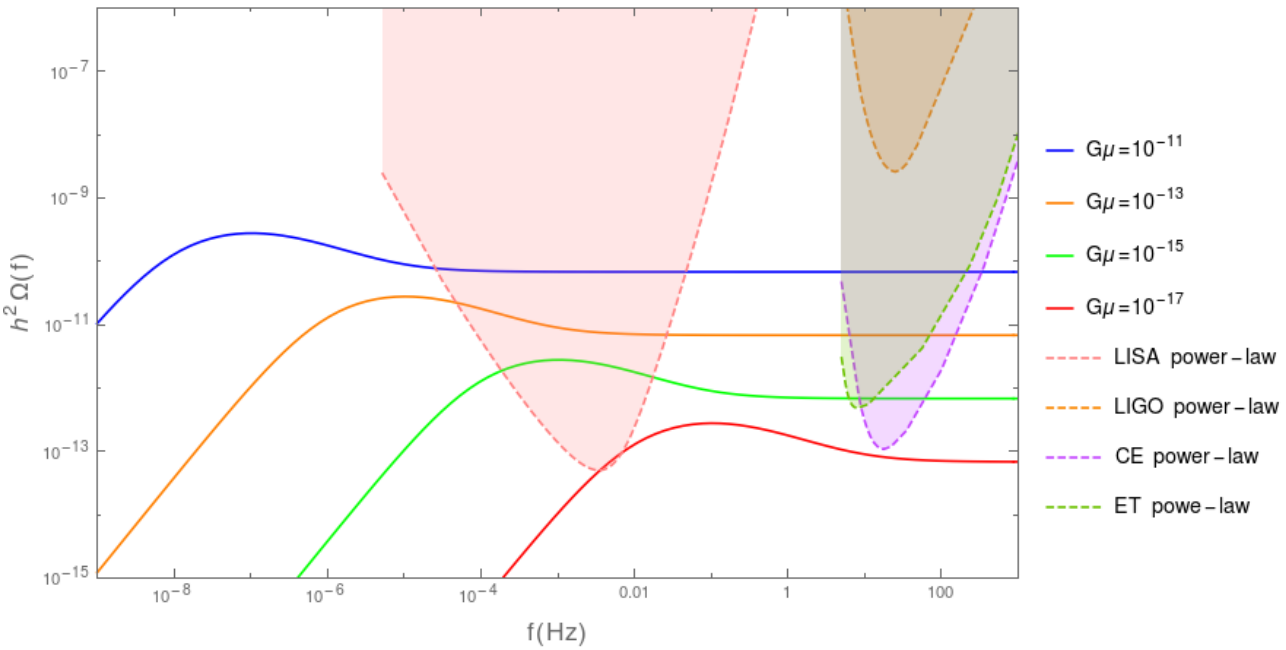

Figure 11: We set $t_F \to 0$ and vary the value of $G\mu$. All the detectors have $SNR = 20$ and $t = 5$ years.

detectors CE and ET, see Figs. 12 and 11. Note that the turn-over at larger frequencies seen in Fig. 12 depends on the network formation temperature at time t_F. The smaller the temperature the earlier we can see this turn-over in the behaviour.

6 Conclusions

The cosmological stochastic GW backgrounds presented in this report can be modelled with a power-law. We have shown that the detection sensitivity increases when we take into account integrating over frequency in addition to time.

We have taken a closer look into two sources of relic GWs that may contribute to the stochastic background, cosmological first-order phase transitions and cosmic strings. The models considered in this report clearly show that LISA is sensitive to both of these sources, see Figs. 7 and 11 and may thus probe the cosmology of the very early universe. In addition, both CE and ET are sensitive to a background from cosmic strings. However, this heavily depends on the string tension of the cosmic strings. Currently the strongest bounds come from PTA data and in the future we will be able to set even more stringent limits.

Acknowledgements

I would like to express my gratitude towards my supervisors Géraldine Servant and Valerie Domcke for their support and fruitful discussions during these eight weeks. I would also like to thank Iason Baldes and Yann Gouttenoire for their help. Big thanks for my summie colleague Sam Wikeley. Last but not least I would like to extend my thanks to the other summies, especially to the people from kitchen 2A for making this summer one of the most memorable ones of my life.

References

[1] B. P. Abbott et al. GW150914: Implications for the stochastic gravitational wave background from binary black holes. *Phys. Rev. Lett.*, 116(13):131102, 2016.

[2] M.H. Poincaré. Sur la dynamique de l'électron. *Rend. Circ. Matem. Palermo*, 21:129–175, 1906.

[3] George Hobbs and Shi Dai. A review of pulsar timing array gravitational wave research. 2017.

[4] `https://www.skatelescope.org/`. Accessed: 2018-09-05.

[5] Michele Maggiore. Gravitational wave experiments and early universe cosmology. *Phys. Rept.*, 331:283–367, 2000.

[6] Eric Thrane and Joseph D. Romano. Sensitivity curves for searches for gravitational-wave backgrounds. *Phys. Rev.*, D88(12):124032, 2013.

[7] Chiara Caprini et al. Science with the space-based interferometer eLISA. II: Gravitational waves from cosmological phase transitions. *JCAP*, 1604(04):001, 2016.

[8] `https://www.lisamission.org/`. Accessed: 2018-09-05.

[9] K. Kajantie, M. Laine, K. Rummukainen, and Mikhail E. Shaposhnikov. Is there a hot electroweak phase transition at m(H) larger or equal to m(W)? *Phys. Rev. Lett.*, 77:2887–2890, 1996.

[10] Margot Fitz Axen, Sharan Banagiri, Andrew Matas, Chiara Caprini, and Vuk Mandic. Multi-wavelength observations of cosmological phase transitions using LISA and Cosmic Explorer. 2018.

[11] David J. Weir. Gravitational waves from a first order electroweak phase transition: a brief review. *Phil. Trans. Roy. Soc. Lond.*, A376(2114):20170126, 2018.

[12] M. B. Hindmarsh and T. W. B. Kibble. Cosmic strings. *Rept. Prog. Phys.*, 58:477–562, 1995.

[13] A. Vilenkin and E.P.S Shellard. *Cosmic strings and other topological defects.* Cambridge University Press, 1994.

[14] Xavier Siemens, Vuk Mandic, and Jolien Creighton. Gravitational wave stochastic background from cosmic (super)strings. *Phys. Rev. Lett.*, 98:111101, 2007.

[15] Sachiko Kuroyanagi, Takeshi Chiba, and Tomo Takahashi. Probing the Universe through the Stochastic Gravitational Wave Background. 2018.

[16] Neil Andrew Bevis. *Constraints on topological defects using the cosmic microwave background radiation.* PhD thesis, University of Sussex, 2005.

[17] Yanou Cui, Marek Lewicki, David E. Morrissey, and James D. Wells. Cosmic Archaeology with Gravitational Waves from Cosmic Strings. *Phys. Rev.*, D97(12):123505, 2018.

[18] Yanou Cui, Marek Lewicki, David E. Morrissey, and James D. Wells. Probing the pre-BBN universe with gravitational waves from cosmic strings. 2018.

A Appendix

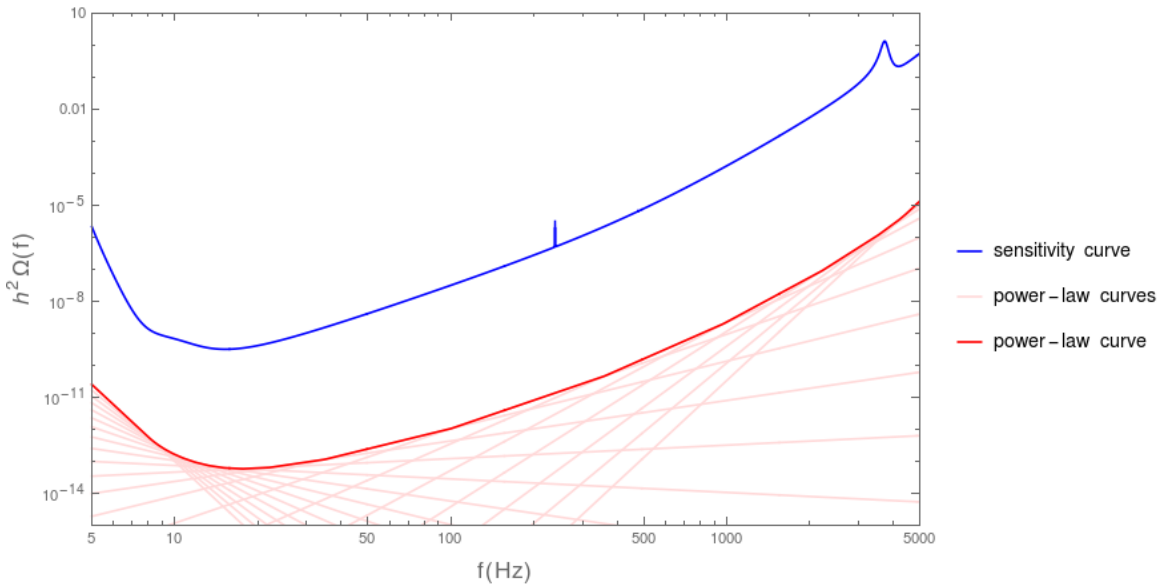

Figure 12: CE with $SNR = 10$ and $t = 4$ years.

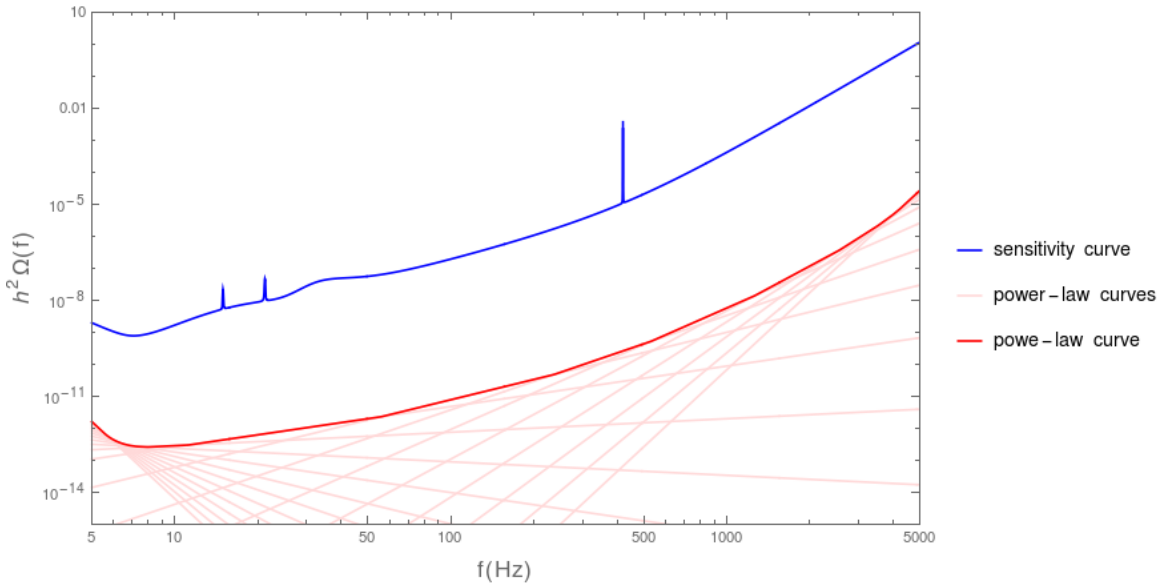

Figure 13: ET with SNR=10 and $t = 4$ years.